© 2022. Published by The Company of Biologists Ltd | Journal of Cell Science (2022) 135, jcs260014. doi:10.1242/jcs.260014

RESEARCH ARTICLE

Identification of a stretch of four discontinuous amino acids involved in regulating kinase activity of IGF1R

Aadil Qadir Bhat[1,2,*], Mir Owais Ayaz[1,2,*], Razak Hussain[3,*], Mohmmad Saleem Dar[2], Md Mehedi Hossain[1,2], Farheen Showket[1,2], Mohd Saleem Dar[4], Yusuf Akhter[5] and Mohd Jamal Dar[1,2,‡]

ABSTRACT

IGF1R is pursued as a therapeutic target because of its abnormal expression in various cancers. Recently, we reported the presence of a putative allosteric inhibitor binding pocket in IGF1R that could be exploited for developing novel anti-cancer agents. In this study, we examined the role of nine highly conserved residues surrounding this binding pocket, with the aim of screening compound libraries in order to develop small-molecule allosteric inhibitors of IGF1R. We generated GFP fusion constructs of these mutants to analyze their impact on subcellular localization, kinase activity and downstream signaling of IGF1R. K1055H and E1056G were seen to completely abrogate the kinase activity of IGF1R, whereas R1064K and L1065A were seen to significantly reduce IGF1R kinase activity. During molecular dynamics analysis, various structural and conformational changes were observed in different conserved regions of mutant proteins, particularly in the activation loop, compromising the kinase activity of IGF1R. These results show that a stretch of four discontinuous residues within this newly identified binding pocket is critical for the kinase activity and structural integrity of IGF1R.

This article has an associated First Person interview with the first author of the paper.

KEY WORDS: PI3K signaling, AKT, IGF1R signaling, ERK, MAPK pathway, Allosteric inhibitors

INTRODUCTION

Insulin-like growth factor receptor (IGF1R) is a transmembrane receptor tyrosine kinase (RTK) that belongs to the insulin receptor family (Li et al., 2019). IGF1R consists of an extracellular ligand-binding domain and an intracellular tyrosine kinase domain (Yuan et al., 2018). The three ligands – IGF1, IGF2 and insulin, with a common three-dimensional structure, have been shown to bind to IGF1R and insulin receptor (IR; also known as INSR) with different affinities. IGF1 and IGF2 bind to IGF1R with high affinity, whereas insulin binds to IR with high affinity (Torres et al., 1995). When a ligand binds to the extracellular α-subunit, it triggers conformational changes in the receptor that cause autophosphorylation of tyrosine residues (Y1131, Y1135 and Y1136) in the cytoplasmic domain of the β-subunit. This leads to IGF1R activation, which in turn activates intracellular signaling pathways, such as the phosphoinositide-3-kinase (PI3K) and mitogen-activated protein kinase (MAPK) pathways (Hakuno and Takahashi, 2018). IGF1R and IR belong to the same RTK family. IR and IGF1R have a high degree of sequence and structural homology, particularly in their intracellular kinase domain and the ATP-binding region, which show nearly 100% sequence similarity. Despite the high degree of sequence and structural similarity, IGF1R and IR exhibit divergent activities (Girnita et al., 2014). Whereas IR is necessary for glucose homeostasis (Bedinger and Adams, 2015), IGF1R is important for cell growth, survival, migration and differentiation, and its dysregulation has been linked to a variety of malignancies (Farabaugh et al., 2015; Werner and Bruchim, 2009). Recently, IR and IGF1R have been reported to translocate into the nucleus of many cell types and shown to be involved in modulating TCF-dependent Wnt–β-catenin signaling activity (Deng et al., 2011; Jamwal et al., 2018; Mills et al., 2021; Packham et al., 2015; Sehat et al., 2010).

Owing to the high degree of homology between IGF1R and IR, tyrosine kinase inhibitors designed against IGF1R are inevitably targeting IR as well (Boone and Lee, 2012; Simpson et al., 2017). As a result, these IGF1R inhibitors are involved in impairing glucose homeostasis, leading to hyperglycemia (Goldman et al., 2016; King and Wong, 2012; Yin et al., 2013). This selectivity issue associated with kinase inhibitors is shifting focus to the development of highly selective protein-specific small molecules. Thus, the identification and development of allosteric small-molecule IGF1R inhibitors is pursued with great interest, although finding allosteric inhibitor binding sites are proving very daunting in this complex kinase. A prior study from our group showed the presence of a putative allosteric inhibitor binding pocket in IGF1R (Jamwal et al., 2018). Furthermore, we identified a conserved residue K1055, surrounding this pocket, involved in regulating the kinase activity of IGF1R. *In silico* analysis showed that this binding pocket is surrounded by conserved residues such as W992, K1055, E1056, F1057, N1058, C1059, H1060, R1064, L1065, Q1071, I1078I and T1083 (Bano et al., 2020; Jamwal et al., 2018).

In this study, we examined the impact of these conserved residues on various activities of IGF1R and its downstream signaling, and identified critical residues (K1055H, E1056G, R1064K and L1065A) involved in regulating the kinase activity and structural integrity of IGF1R.

RESULTS

Expression and activity analysis of critical conserved residues surrounding allosteric inhibitor binding pocket of IGF1R

Recently, we reported the presence of a unique allosteric inhibitor binding pocket in IGF1R and a critical residue, K1055, within this region involved in regulating the kinase activity of IGF1R (Jamwal

[1]Academy of Scientific and Innovative Research, Ghaziabad, Uttar Pradesh 201002, India. [2]Cancer Pharmacology Division, Council of Scientific and Industrial Research-Indian Institute of Integrative Medicine, Jammu, Jammu and Kashmir 180001, India. [3]Department of Botany, Central University of Jammu, Rahya Suchani, Jammu and Kashmir 181143, India. [4]Department of Biochemistry, Purdue University, West Lafayette, IN 47907, USA. [5]Department of Biotechnology, Babasaheb Bhimrao Ambedkar University, Lucknow, Uttar Pradesh 226025, India.
*These authors contributed equally to this work

‡Author for correspondence (jamal@iim.ac.in)

A.Q., 0000-0002-1390-408X; M.S.D., 0000-0001-8244-6900

Handling Editor: John Heath
Received 15 March 2022; Accepted 3 June 2022

Journal of Cell Science (2022) 135, jcs260014. doi:10.1242/jcs.260014

et al., 2018). Moreover, we showed that this unique binding pocket is surrounded by different conserved residues, which include W992, K1055, E1056, F1057, N1058, C1059, H1060, R1064, L1065, Q1071, I1078I and T1083. Here, we performed a multiple sequence alignment and observed that all the residues within this stretch of IGF1R are highly conserved across eight different species; however, all these residues are not conserved between IGF1R and IR. E1056, N1058, Q1071 and T1083 in IGF1R are replaced by G1080, T1082, K1094 and A1106 in IR (Fig. 1A). In order to examine the role of highly conserved residues on the various activities of IGF1R, we generated mutants of selected residues (E1056G, F1057Y, C1059A, H1060A, R1064K, L1065A, Q1071K, I1078V and T1083A), on the basis of *in silico* analysis, and expressed these proteins in HEK-293 cells. Immunoblot analysis using GFP-specific antibodies showed that all these proteins are expressed at the expected size (Fig. 1B,E). On examining the autophosphorylation activity of these mutants in comparison to wild type (WT), K1055R mutant and GFP vector control, a significant decrease was seen in E1056G, R1064K and L1065A mutants. E1056G completely abrogated the kinase activity of IGF1R, and L1065A and R1064K induced a significant decrease in IGF1R kinase activity; all other mutants had no effect on IGF1R kinase activity (Fig. 1F–I). Furthermore, we investigated the subcellular location of E1056G, R1064K and L1065A mutants using confocal microscopy in HEK-293 cells. E1056G, R1064K and L1065A mutants were seen to be predominantly present at the cell surface, with some presence in the cytoplasm and nucleus as well, in a fashion similar to IGF1R WT, indicating that these mutations do not affect the subcellular localization of IGF1R (Fig. 1J).

Downstream signaling activity of IGF1R point mutations

Ligand binding to extracellular domain induces autophosphorylation of IGF1R, which in turn activates downstream signaling through PI3K and MAPK pathways in order to promote cell growth, proliferation and survival. Increased levels of phosphorylated

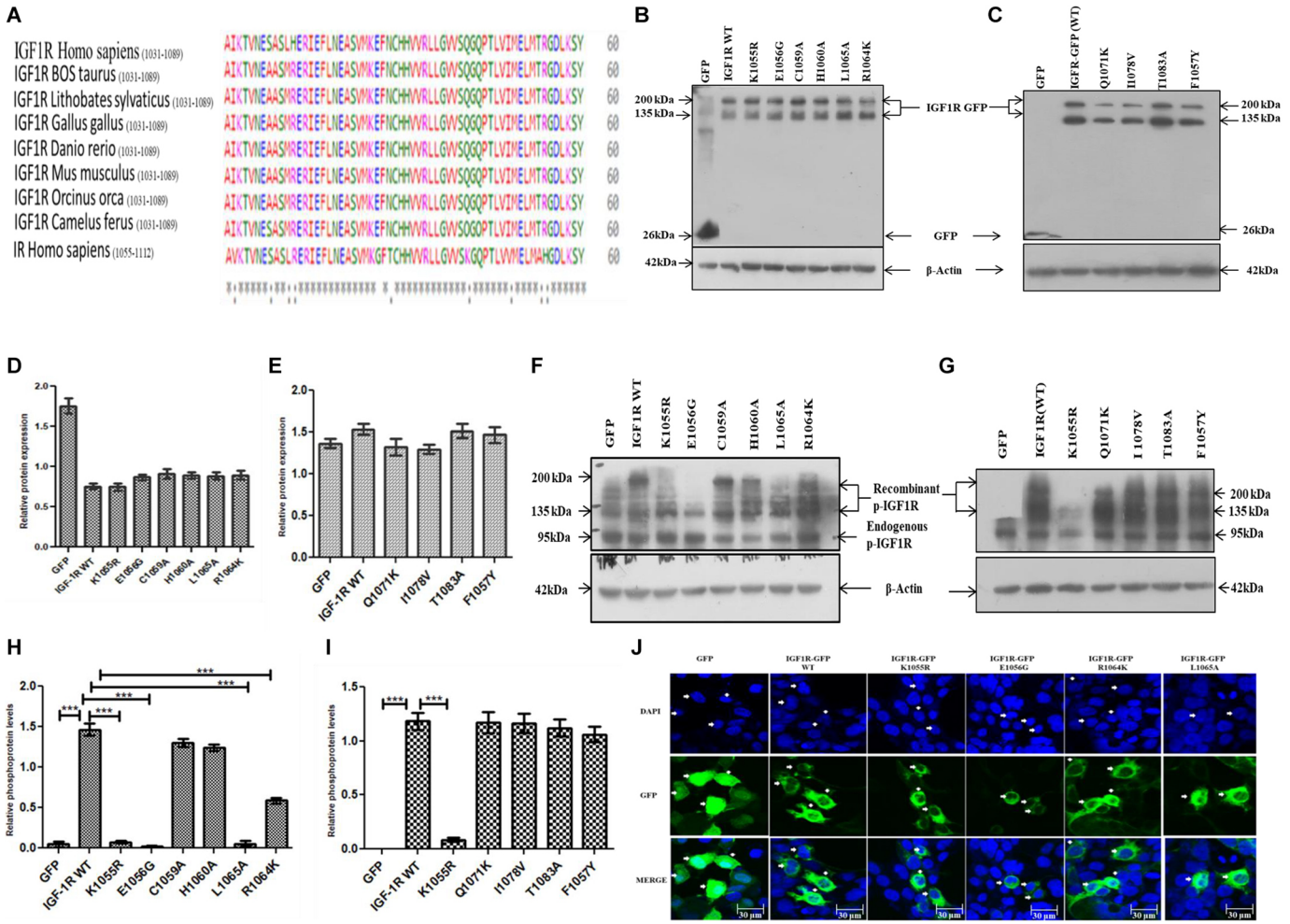

Fig. 1. Expression and localization of IGF1R–GFP (WT) and its point mutations in HEK-293 cells. (A) Sequence alignment of residues surrounding the putative allosteric inhibitor binding pocket. The sequence alignment was performed between eight different species, including *Homo sapiens* (human), *Bos taurus* (cow), *Lithobates sylvaticus* (wood frog), *Gallus gallus* (red jungle fowl), *Danio rerio* (zebrafish), *Mus musculus* (house mouse), *Orcinus orca* (killer whale) and *Camelus ferus* (Bactrian camel) using Clustal Omega. (B,C) HEK-293 cells were transiently transfected with GFP, IGF1R–GFP (WT), K1055R, E1056G, C1059A, H1060A, L1065A, R1064K, Q1071K, I1078V, T1083A and F1057Y plasmids to determine their expression by immunoblotting using anti-GFP antibodies. (F,G) Autophosphorylation activity using anti-pIGF1R antibodies. β-actin was used as loading control. (D,E,H,I) Densitometry analysis of GFP and pIGF1R with respect to β-actin and endogenous pIGF1R, respectively. pIGF1R quantitation involves signals from both bands (pro-receptor 200 kDa and mature receptor 135 kDa) with respect to endogenous pIGF1R. (J) Subcellular localization of IGF1R WT and mutant proteins using confocal microscopy at 40× magnification using GFP as control. Arrows indicate nuclear localization of IGF1R and its mutants. Images are representative of three independent experiments. Scale bars: 30 µm. The data shown represent the mean±s.d. of three independent experiments (***P<0.001; one-way ANOVA).

Journal of Cell Science (2022) 135, jcs260014. doi:10.1242/jcs.260014

(p)AKT and pERK (also known as pMAPK) are indicative of PI3K and MAPK pathway activation, respectively. Upon expressing GFP fusion proteins in HEK-293 cells to assess their pAKT and pERK levels using pAKT- and pERK-specific antibodies under serum-free conditions, we observed that E1056G, L1065A and R1064K mutants showed significantly decreased pAKT and pERK levels in comparison to those of WT and K1055R, as expected (Fig. 2A–H).

Generation of double mutants and their expression and activity analysis

Because E1056G, L1065A and R1064K showed considerably decreased levels of kinase activity and downstream signaling, we generated double mutants of these proteins (E1056G/R1064K, E1056G/L1065A and R1064K/L1065A) to further validate their impact on various activities of IGF1R. These double mutants were transfected into HEK-293 cells, and immunoblot analysis was carried out to confirm their expression using GFP-specific antibodies. As expected, all three mutants were expressing at equal levels (Fig. 3A,B). After we established that they were expressing correct size proteins, we analyzed their autophosphorylation activity in HEK-293 cells using pIGF1R-specific antibodies. Double mutations were seen to completely abrogate the kinase activity of IGF1R. Upon transfecting these proteins in HEK-293 cells, we observed a significant decrease in pAKT and pERK levels as well (Fig. 3C–H). These results indicate that E1056, R1064 and L1065 play a pivotal role in regulating the kinase activity of IGF1R protein.

Molecular dynamics analysis of K1055R, E1056G, R1064K, L1065 and their double mutants

Thus far, we had observed that E1056G completely abrogated the kinase activity of IGF1R, and R1064K and L1065A significantly reduced IGF1R kinase activity. Thus, we performed molecular dynamics analysis in order to examine how these mutations may impact the structural integrity of IGF1R (Fig. 4A). Inactivated Apo form of WT IGF1R [Protein Data Bank (PDB) ID: 1M7N] and mutants of critical residues (K1055R, E1056G, R1064K and L1065A) were subjected to molecular dynamics simulations to observe the structural transformations and the stability of each mutant backbone, as analyzed by plotting root mean square deviations (RMSDs), where the RMSD value of the Cα backbone lies within 0.4 nm for single and double mutants (Fig. S1A,C). The root mean square fluctuation (RMSF) value for each amino acid drops from 0.75 nm to 0.2 nm, and from 0.55 nm to 0.25 nm, in WT and mutant proteins, respectively (Fig. S1B,D). The mutants of IGF1R exhibited numerous structural transformations during simulations within and outside of the activation loop. A conformational change was observed in the activation loop of all the mutant proteins, with a drift of 14.9 Å in K1055R, 10.6 Å in E1056G, 7.6 Å in R1064K and 6.9 Å in L1065A for single mutants (Fig. 5F–I; Table S3), and 8.1 Å in E1056G/L1065A, 7.8 Å in E1056G/R1064K and 9.1 Å in L1065A/R1064K for double mutants (Table S4, Fig. S2E–G). This conformational change in the activation loop led to a change in side-chain orientation of conserved tyrosine residues (Y1158, Y1162 and Y1163) involved in the autophosphorylation activity of IGF1R (Pautsch et al., 2001). We reported earlier that K1055R mutation causes many structural changes in the IGF1R protein (Jamwal et al., 2018). In-depth analyses showed that K1055R exhibited structural changes of loop to α-helix at V1173–M1176 and at I1263–E1266 near the activation loop and C-terminal, respectively, and loop to β-sheet at R1081–L1084 in the hinge region during simulation (Fig. 4B,F). The structural transformations were observed for mutant E1056G from α-helix to loop at I1157–R1164 in the activation loop, from loop to α-helix at I1263–E1266 near the C-terminal, and from loop to β-sheet at I996–R1000 near the ATP-binding region (Fig. 4C,G). The structural changes observed for mutant R1064K were from α-helix to loop at I1157–R1164 in the activation loop, from loop to α-helix

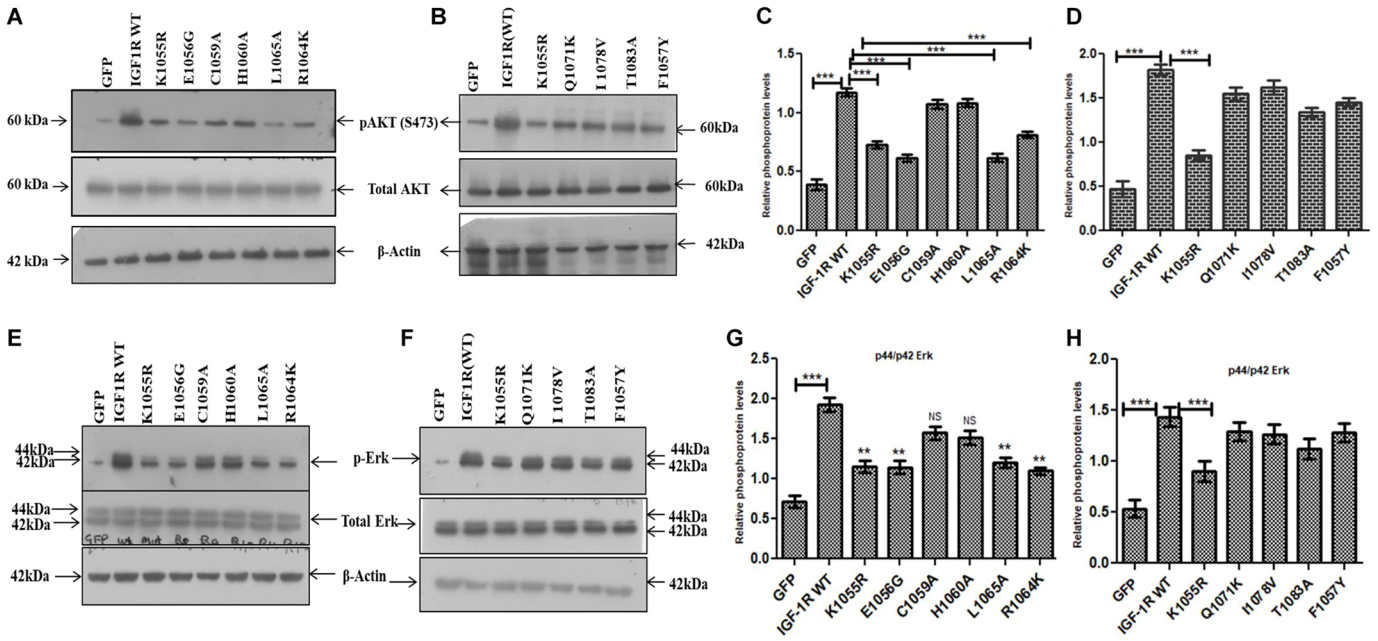

Fig. 2. Effect of IGFR–GFP (WT), K1055R and nine other point mutations in HEK-293 cells on downstream signaling. (A–H) Immunoblotting of HEK-293 cells transiently transfected with GFP, IGF1R–GFP (WT), K1055R, E1056G, C1059A, H1060A, L1065A, R1064K, Q1071K, I1078V, T1083A and F1057Y to determine their effect on downstream signaling using anti-pAKT and anti-pERK antibodies. Total AKT and total ERK was used as expression control for pAKT and pERK, respectively. β-actin was used as loading control. (C,D,G,H) Densitometry analysis of western blot experiments for pAKT with respect to total AKT (C,D) and pERK with respect to total ERK (G,H). The data shown represent the mean±s.d. of three independent experiments (**P<0.01, ***P<0.001; one-way ANOVA).

Journal of Cell Science (2022) 135, jcs260014. doi:10.1242/jcs.260014

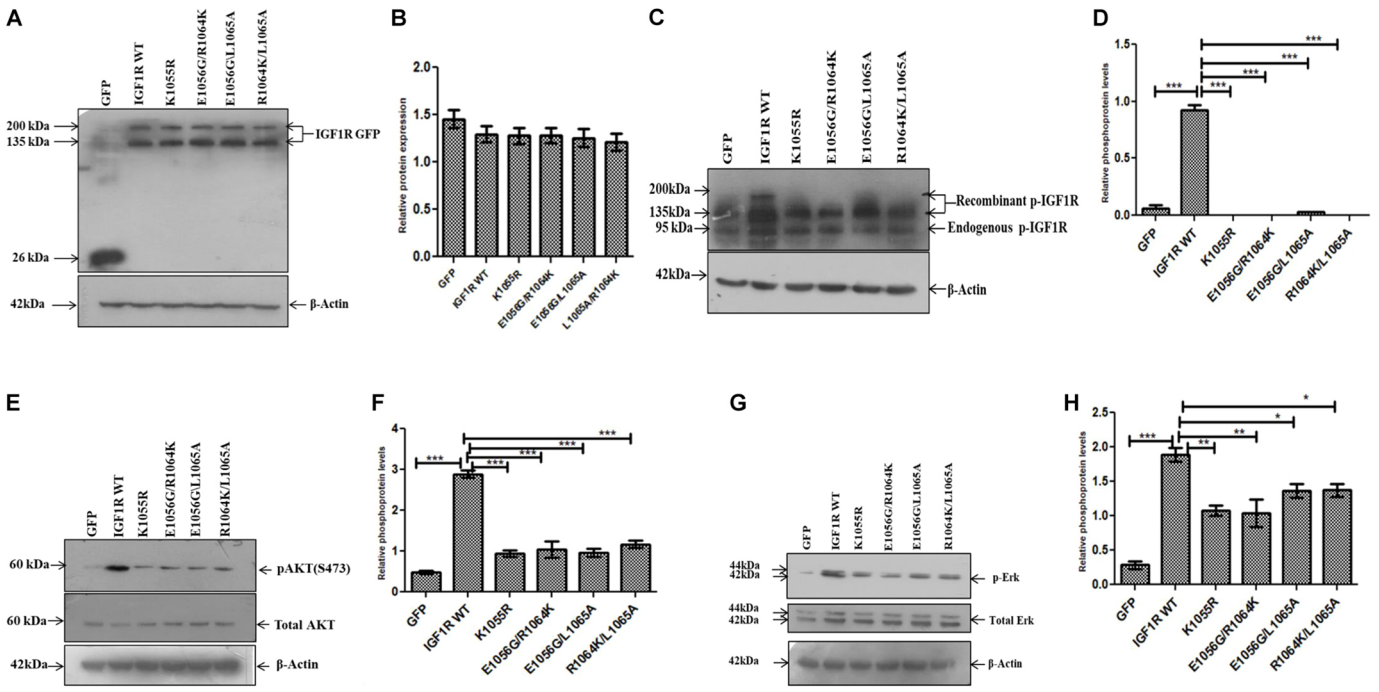

Fig. 3. Expression and activity analysis of IGF1R, K1055R and double mutants. (A) HEK-293 cells were transiently transfected with GFP, IGF1R WT, K1055R, E1056G/R1064K, E1056G/L1065A and R1064K/L1065A plasmids to determine their expression by immunoblotting using anti-GFP antibody. (C) Autophosphorylation activity using anti-pIGF1R antibody. (E,G) Effect on downstream signaling using anti-pAKT and anti-pERK antibodies. β-actin was used as loading control. (B,D,F,H) Densitometry analysis of GFP (B), recombinant pIGF1R with respect to endogenous pIGF1R. pIGF1R quantitation involves signals from both bands (pro-receptor 200 kDa and mature receptor 135 kDa) with respect to endogenous pIGF1R (D), pAKT with respect to total Akt (F), and pERK with respect to total ERK (H). The data shown represent the mean±s.d. of three independent experiments (NS, not significant; **P*<0.05, ***P*<0.01, ****P*<0.001; one-way ANOVA).

at V1173–M1176 near the activation loop, and from loop to β-sheet at I996–R1000 near the ATP-binding region (Fig. 4D,H). The structural transformations observed for mutant L1065A were from α-helix to loop at I1157–R1164 and at V1173–M1176 in the activation loop and near to the activation loop, from loop to α-helix at I1263–E1266 near the C-terminal, from loop to β-sheet at K1165–L1171 in the activation loop, and from β-sheet to loop at C1138–I1148 (Fig. 4E–I).

Similarly, structural transformations were also observed for double mutants during simulation. For mutant E1056G/L1065A, the structural changes observed were from α-helix to loop at R993–I996, I1157–R1164 and P1269–V1274 near the ATP-binding region, in the activation loop and near the C-terminal, from loop to α-helix at N1033-A1036 near the αC-helix, and from β-sheet to loop at C1138–I1148 near the catalytic loop (Fig. S2B,E). The structural changes observed for mutant E1056G/R1064K were from loop to β-sheet at R1081–L1084 in the hinge region (Fig. S2C,F), and the structural changes observed for mutant L1065A/R1064K were from α-helix to loop at R993–I996, I1157–R1164 and P1269–V1274 near the ATP-binding region, in the activation loop and near the C-terminal, from loop to α-helix at N1249–M1252, and from loop to β-sheet at R1081–L1084 in the hinge region (Fig. S2D,G). Thus, we observed the presence of a binding pocket that lies next to the αC-helix consisting of W992, K1055, E1056, F1057, N1058, C1059, H1060, R1064, L1065, Q1071, I1078I and T1083; this is consistent with our earlier report (Bano et al., 2020). A similar type of pocket has also been reported in human ephrin RTK (PDB ID: 2QON) (Carrasco-García et al., 2014). These conformational changes in the activation loop and the various structural transformations observed within the conserved regions of IGF1R in different mutants may lead to distortion in orientation of tyrosine residues in the activation loop, which could result in disruption of the kinase activity of IGF1R. The double mutants showed additional structural changes compared to single mutants, which validates the results we obtained using *in vitro* assays.

Impact of K1055 substitution mutations on IGF1R kinase activity and downstream signaling

Because the K1055R mutant was shown to abrogate the kinase activity of IGF1R (Jamwal et al., 2018), we generated six substitution mutations of K1055 (K1055A, K1055G, K1055T, K1055H, K1055E and K1055Q) in order to examine their impact on IGF1R activity, with the aim of identifying small molecules that can fit into this pocket. HEK-293 cells were transfected with the plasmids encoding GFP-tagged IGF1R WT, K1055R and the six substitution mutants of K1055. Immunoblots were probed with GFP-specific antibodies, and expression of expected size proteins was observed (Fig. 5A,B). Upon assessing the kinase activity of these mutants in comparison to WT IGF1R and K1055R mutant, K1055H was seen to drastically reduce the kinase activity of IGF1R in a similar manner to K1055R. K1055A, K1055T, K1055G and K1055Q mutants were observed to moderately decrease IGF1R kinase activity, whereas K1055E did not affect IGF1R kinase activity (Fig. 5C,D). K1055H resulted in a significant decrease in pAKT and pERK levels as well (Fig. 5E–H). Furthermore, we performed computational molecular dynamics analysis to examine the effect of K1055H on the structural integrity of IGF1R. The RMSD values for each amino acid dropped from 0.6 nm to 0.4 nm, and from 0.2 nm to 0.15 nm, in IGF1R WT and K1055H, respectively. Structural changes observed in K1055H showed a drift of 11.4 Å in the activation loop when compared with WT IGF1R. In K1055H mutant, structural changes from loop to α-

Journal of Cell Science (2022) 135, jcs260014. doi:10.1242/jcs.260014

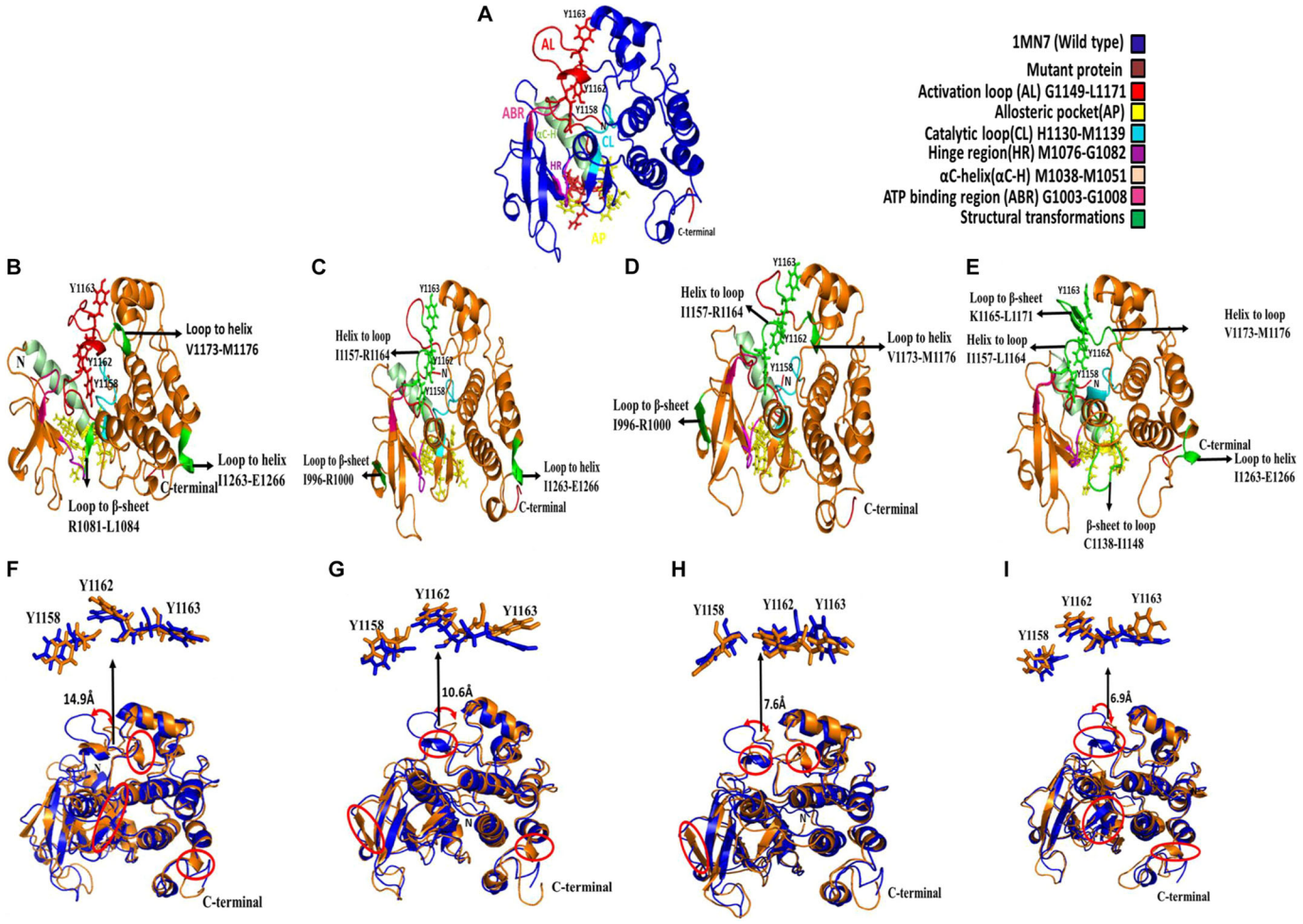

Fig. 4. Structural transformations in IGF1R mutants in comparison to WT IGF1R protein. The structure of WT IGF1R protein can be seen in PDB ID: 1M7N. (A) Conserved regions of IGF1R represented in different colors (IM7N WT, blue; mutant proteins, brown; activation loop (AL), red; allosteric pocket (AP), yellow; catalytic loop (CL), cyan; hinge region (HR), violet; αC-helix (αC-H), pale pink; ATP-binding region (ABR), magenta; structural transformations, green; conserved tyrosine residues (Y1158, Y1162, Y1163) in activation loop are represented by sticks. (B–E) Structural changes in mutants K1055R (B), E1056G (C), R1064K (D) and L1065A (E). (F,G,H,I) Aligned structure of mutants K1055R (F), E1056G (G), R1064K (H) and L1065A (I) acquired after simulation with IGF1R WT (PDB ID: 1M7N). The structural changes are represented in red circles in aligned figures and drift of activation loop in Å; the side-chain orientation of conserved tyrosine residues is also shown.

helices (R1250–R1253 and A1134–N1137) and loop to β-sheet (R1081–L1084) were observed in the tyrosine kinase domain, catalytic loop and at the end of the hinge region, respectively (Fig. 5I). The non-bonded interaction analysis for K1055 and six point mutations showed that, in K1055H mutant, all interactions are retained, like native IGF1R, except a new hydrophobic interaction that formed between H1055 and L1065, which keeps N- and C-terminal domains apart (Table S2). All these structural changes and new hydrophobic interactions account for the decreased kinase activity of K1055H mutant.

DISCUSSION

IGF1R and IR are two closely related transmembrane RTKs sharing a high degree of sequence and structural homology. The ligand-binding domains of IGF1R and IR show nearly 55% similarities, whereas β-domains show nearly 72% similarities, and the ATP-binding domains show 100% sequence similarity. Despite a high degree of homology, IGF1R and IR perform distinct cellular and physiological functions. Whereas IGF1R is involved in promoting cell growth, proliferation, differentiation, survival, and the self-renewal and pluripotency of stem cells, IR is primarily involved in the regulation of glucose homeostasis. In several types of human cancers, activation of IGF1R-mediated signaling promotes tumor development, metastasis and drug resistance (Hua et al., 2020; Lin et al., 2017; Ngo et al., 2021). Because of the high degree of sequence and structural homology between IGF1R and IR, it is difficult to target IGF1R-mediated signal transduction in cancer cells (Ullrich et al., 1986). This is one of the primary reasons why IGF1R-specific small molecules fail to reach to advanced clinical stages. Scientists believe that when the natural active sites of a target protein are not amenable to drug development, allosteric inhibitor binding pockets provide the most tenable alternative to perturb the function of target protein. However, identification of allosteric sites in these proteins is a daunting task. Recently, we identified a novel allosteric inhibitor binding pocket in IGF1R and a highly conserved lysine residue (K1055) within this pocket involved in regulating autophosphorylation as well as the downstream signaling activity of IGF1R (Jamwal et al., 2018). In the present study, we explored the impact of various conserved residues on various activities of IGF1R, with the aim of characterizing this binding pocket in order to screen compound libraries to identify small molecules that can fit into this pocket to act as allosteric inhibitors for the treatment of

Journal of Cell Science (2022) 135, jcs260014. doi:10.1242/jcs.260014

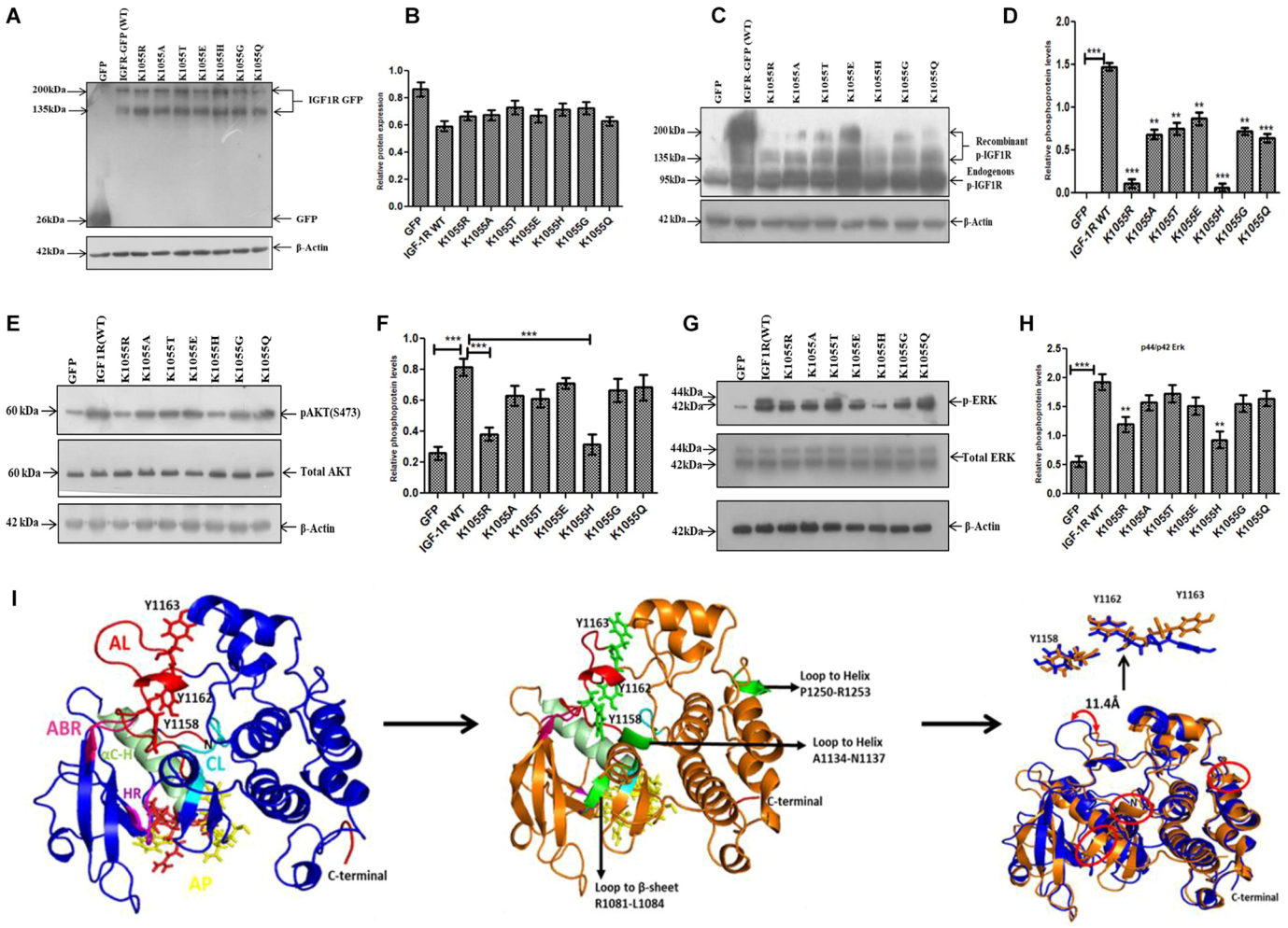

Fig. 5. Expression and activity analysis of K1055 and its substitution mutants. (A) HEK-293 cells were transiently transfected with GFP, IGF1R–GFP (WT), K1055R, K1055A, K1055G, K1055T, K1055H, K1055E and K1055Q plasmids to determine their expression by immunoblotting using anti-GFP antibodies. (C) Autophosphorylation levels of WT and IGF1R mutants using anti-pIGF1R antibodies. (E,G) Effect on downstream signaling using anti-pAKT and anti-pERK antibodies. β-actin was used as loading control. (B,D,F,H) Densitometry analysis of GFP (B), recombinant pIGF1R with respect to endogenous pIGF1R. pIGF1R quantitation involves signals from both bands (pro-receptor 200 kDa and mature receptor 135 kDa) with respect to endogenous pIGF1R (D), pAKT with respect to total AKT (F), and pERK with respect to total ERK (H). (I) Representation of the aligned structure of mutant K1055H obtained after simulation and the IGF1R WT (PDB ID: 1M7N), with structural changes in red circles and drift of activation loop in Å; the side-chain orientation of conserved tyrosine residues is also represented by sticks. All data shown represent the mean±s.d. of three independent experiments (***P*<0.05, ****P*<0.001; one-way ANOVA).

IGF1R signaling-mediated malignancies. To begin with, we generated point mutations of nine highly conserved residues (E1056G, C1059A, H1060A, L1065A, R1064K, Q1071K, I1078V, T1083A and F1057Y) surrounding this allosteric inhibitor binding pocket. During immunoblot analysis, all these mutant proteins were seen to be expressing at the correct size when compared to WT IGF1R protein. Confocal microscopy analysis was performed to examine the subcellular localization of these proteins, and all the mutant proteins were seen to be present at the membrane, in the cytoplasm and nucleus, in a manner akin to that of the WT protein. We then carried out activity analysis of these mutants in comparison to WT and vector control in HEK-293 cells. E1056G, R1064K and L1065A mutants were seen to drastically reduce the autophosphorylation activity of IGF1R. Interestingly, E1056G was seen to completely abrogate the IGF1R kinase activity compared to WT IGF1R protein. We also assessed the activation of PI3K and MAPK signaling pathways by analyzing pAKT and pERK levels upon expressing these proteins in HEK-293 cells. We observed that E1056G, R1064K and L1065A mutants showed significantly reduced levels of pAKT and pERK levels as well.

Furthermore, we generated double mutations to validate the impact of E1056G, R1064K and L1065A on the diverse activities of IGF1R. We observed additional structural changes in double mutants compared to single mutants, thus reiterating the critical nature of these residues in regulating kinase activity of IGF1R.

We also generated different substitution mutations of K1055 (K1055A, K1055G, K1055T, K1055H, K1055E, K1055Q) and expressed these proteins in HEK-293 cells to examine their impact on various activities of IGF1R, and observed the expression of stable mutant proteins at the expected size. These substitution mutants showed subcellular localization similar to WT protein and were seen to be present at the membrane, as well as in the cytoplasm and nucleus. Among all the substitution mutants, only K1055H was seen to drastically reduce IGF1R autophosphorylation activity, as well as pAKT and pERK levels, compared to WT and K1055R under similar conditions.

During *in silico* analysis, we observed many structural changes occurring in different conserved regions, particularly in the activation loop of these mutants. As a result of these structural changes, critical

Journal of Cell Science (2022) 135, jcs260014. doi:10.1242/jcs.260014

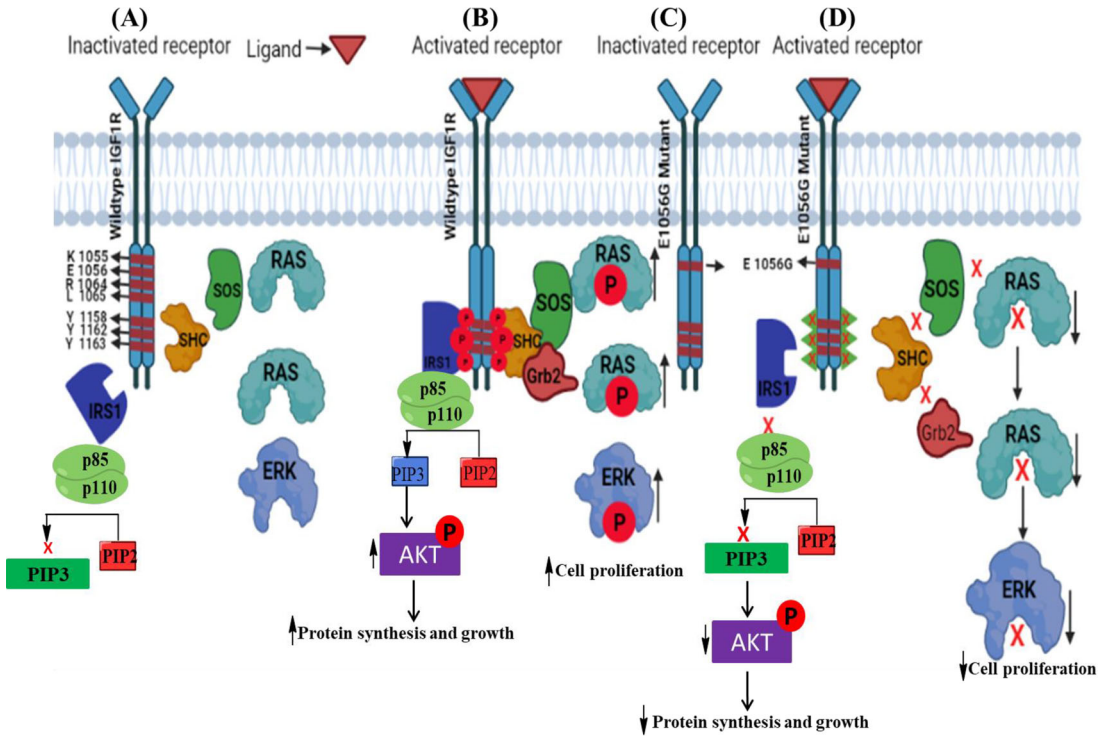

Fig. 6. Model depicting the impact of E1056G mutation on IGF1R-mediated signaling. Mutation of selected residues (K1055H, R1064K, L1065A and E1056G) within this putative allosteric inhibitor binding pocket was seen to either completely abrogate IGF1R kinase activity or significantly reduce it. (A,B) The model shows IGF1R-mediated signaling when the ligand is not bound (A), and when the ligand is bound and receptor is activated by autophosphorylation of its three cognate tyrosine residues resulting in downstream activation of PI3K and MAPK signaling (B). E1056G mutation abrogates the phosphorylation of three critical tyrosine residues (Y1158, Y1162 and Y1163), thereby reducing the autophosphorylation activity of IGF1R and resulting in decreased phosphorylation of its effector proteins (pAKT and pERK), which are indicative of PI3K and MAPK activation (C), and thus impacting the physiological activities of IGF1R (D). P, phosphorylated; PIP2, phosphatidylinositol 4,5-bisphosphate; PIP3, phosphatidylinositol (3,4,5)-trisphosphate.

tyrosine residues (Y1158, Y1162 and Y1163) present in the activation loop showed altered orientation when compared with WT (IM7N) structure. These structural changes may be contributing to the abrogation of autophosphorylation as well as the downstream activities of IGF1R. Based on these findings, here we present the possible effect of one of these mutations (E1056G) on IGF1R activity and its main physiological functions in a model (Fig. 6).

In conclusion, we identified a stretch of four discontinuous residues involved in regulating the kinase activity of IGF1R. These critical residues are highly conserved among various species of IGF1R and are part of a newly identified allosteric inhibitor binding pocket in IGF1R. Our study results suggest that this region is involved in mediating various activities of IGF1R through interactions with yet to be identified proteins in the cell, thus could be exploited for developing IGF1R-specific allosteric small-molecule inhibitor(s). The mutation analysis was carried out as a part of a larger plan to examine the exact role of highly conserved amino acids in this newly identified binding pocket to screen compound libraries for the identification of small molecules that can fit into this pocket and specifically target IGF1R only.

MATERIALS AND METHODS

Plasmids

IGF1R human cDNA was kindly provided by Dusty Miller [Fred Hutchinson Cancer Research (FHCRC), Seattle, Washington 98104, USA]. A site-directed mutagenesis kit (Thermo Fisher Scientific) was used to produce point mutations in IGF1R using different primers (MJ151–MJ174) for generating different mutations such as glutamate to glycine (E1056G), phenylalanine to tyrosine (F1057Y), cysteine to alanine (C1059A), histidine to alanine (H1060A), arginine to lysine (R1064K), glutamine to lysine (Q1071K), isoleucine to valine (I1078V), threonine to alanine (T1083A) and leucine to alanine (L1065A). For details of primers used in site-directed mutagenesis, see Table S1.

Cell lines, transfection

We used a normal transformed HEK-293 cell line obtained from the National Center for Cell Science (NCCS), Pune, India. Dulbecco's modified Eagle medium (DMEM; Sigma-Aldrich, D7777) was used to culture and maintain HEK-293 cells in 75 cm^3 flasks supplemented with 10% fetal bovine serum (FBS; qualified, standard origin Brazil; GIBCO, 10270106). Lipofectamine 2000 (Invitrogen) was used as the transfection reagent.

Antibodies and reagents

Anti-pIGF1R (sc-135767) and anti-GFP (sc-9996) antibodies were purchased from Santa Cruz Biotechnology. Monoclonal anti β-actin (A5441) antibody was purchased from Sigma-Aldrich. Anti-total AKT (C67E7), anti-pAKT (S473) (D9E), anti-total ERK (9102S), anti-pERK (9101S) anti-rabbit (7074P2) and anti-mouse (7076S) antibodies were purchased from Cell Signaling Technology. Antibodies were used at 1:1000 dilutions. All other reagents and chemicals used were obtained from Sigma-Aldrich.

SDS-PAGE and western blotting

HEK-293 cells were seeded in six-well plates at a density of 0.5×10^6 per well. Two micrograms of GFP-fused IGF1R (WT) and its different

constructs were transiently transfected into HEK-293 cells using Lipofectamine (4 µl) as transfecting reagent after 24 h of cell seeding. After transfection, cells were grown in Opti-MEM (Thermo Fisher Scientific, 31985070) for 4–5 h, and then complete medium was added to each well for 24 h. Cells were then lysed using 1× RIPA buffer (Cell Signaling Technology, 9806) along with NAF (100 mM), PMSF (100 mM), protease (Sigma-Aldrich, P2714) and phosphatase inhibitor (Sigma-Aldrich, P0044). Bradford assay was used for the estimation of protein. Equal amounts of proteins were loaded along with the marker protein (Thermo Scientific, 26619), separated by 8%, 10% and 12% SDS-PAGE, and transferred to PVDF membrane (Millipore: 88518). Specific antibodies were used for probing the PVDF membrane and then visualized using Chemiluminescent HRP Substrate (Millipore, WBKLS0100). Raw data for western blots are provided in Fig. S3.

Confocal microscopy

HEK-293 cells were seeded in six-well plates at a density of 25,000 per well in six-well chambered cover glass slides (Thermo Scientific, Lab-Tek 155411). Two micrograms of GFP-fused IGF1R (WT) and its different constructs were transiently transfected in HEK-293 cells using Lipofectamine (4 µl) as transfecting reagent after 24 h of cell seeding. After transfection, cells were grown in Opti-MEM for 4–5 h, and then complete medium was added to each well for 24 h. After 24 h, cells were washed with PBS and then fixed with 4% paraformaldehyde (Sigma-Aldrich, P6148) for 10 min. After fixation, 0.5% Triton X-100 was used for the permeabilization of cells for 10 min, and then cells were stained with 4′,6-diamidino-2-phenylindole (DAPI; Sigma-Aldrich) for 20 min at room temperature. Cells were mounted using mounting medium (glycerol: PBS solution; 9:1) and visualized under a confocal microscope (Olympus Fluoview FV-1000). The magnification used was 40×.

Computational dataset and mutant preparation of IGF1R

The crystal structure of IGF1R (PDB ID: 1M7N) was downloaded from the PDB in its Apo form (Gallois-Montbrun et al., 2002). Four single mutants were prepared for K1055R, E1056G, R1064K and L1065A, and three double mutants were generated for E1056G/L1065A, E1056G/R1064K and L1065A/R1064K using the mutagenesis wizard of PyMol (DeLano, 2002). Each mutant and the Apo protein were energy minimized and subjected to molecular dynamics simulations of 20 ns using the Gromacs tool (Berendsen et al., 1995) at 26.8°C temperature and 100 kPa (atmospheric) pressure to analyze the structural changes and the impact of mutating residues on IGF1R Apo protein.

Densitometry and statistical analysis

The band intensities were quantified using ImageJ software. The relative band intensities were calculated by normalizing against β-actin. Western blot images were processed using ImageJ software. All data were analyzed using Prism software (GraphPad). Paired one-tailed Student's *t*-test and one-way ANOVA were used to evaluate statistics, and $P<0.001$ was considered significant.

Acknowledgements

Aadil Qadir Bhat and Mir Owais Ayaz greatfully acknowladges supprort from University Grants Comission (UGC) for Senior Research Fellowships.
This manuscript represents CSIR-IIIM communication number (CSIR-IIIM/IPR/00364).

Competing interests

The authors declare no competing or financial interests.

Author contributions

Conceptualization: A.Q.B., M.J.D.; Methodology: A.Q.B., M.O.A., R.H., Mohmmad S. Dar., M.M.H., F.S., Mohd S. Dar; Software: A.Q.B., R.H., M.O.A.; Validation: A.Q.B., R.H., M.O.A., Y.A., M.J.D.; Formal analysis: A.Q.B., R.H., M.O.A., Y.A., M.J.D.; Investigation: A.Q.B., R.H., M.O.A., Y.A., M.J.D.; Resources: M.J.D.; Data curation: M.J.D.; Writing original draft: A.Q.B., M.O.A., M.J.D.; Writing review and editing: A.Q.B., M.J.D.; Visualization: A.Q.B., M.J.D.; Supervision: M.J.D.; Project adminstration: M.J.D.; Funding acquisition: M.J.D.

Funding

This work was supported by the Science and Engineering Research Board-Department of Science and Technology, Ministry of Science and Technology, India (EMR/2017/002533) and the Council of Scientific and Industrial Research, India (CSIR-FBR-MLP110007, HCP-0007, HCP-38, HCP-40).

References

Bano, N., Hossain, M. M., Bhat, A. Q., Ayaz, M. O., Kumari, M., Sandhu, P., Akhter, Y. and Dar, M. J. (2020). Analyzing structural differences between insulin receptor (IR) and IGF1R for designing small molecule allosteric inhibitors of IGF1R as novel anti-cancer agents. *Growth Horm. IGF Res.* **55**, 101343. doi:10.1016/j.ghir.2020.101343

Bedinger, D. H. and Adams, S. H. (2015). Metabolic, anabolic, and mitogenic insulin responses: A tissue-specific perspective for insulin receptor activators. *Mol. Cell. Endocrinol.* **415**, 143-156. doi:10.1016/j.mce.2015.08.013

Berendsen, H. J. C., van der Spoel, D. and van Drunen, R. (1995). GROMACS: A message-passing parallel molecular dynamics implementation. *Comput. Phys. Commun.* **91**, 43-56. doi:10.1016/0010-4655(95)00042-E

Boone, D. N. and Lee, A. V. (2012). Targeting the insulin-like growth factor receptor: developing biomarkers from gene expression profiling. *Crit. Rev. Oncog.* **17**, 161-173. doi:10.1615/CritRevOncog.v17.i2.30

Carrasco-García, E., Saceda, M. and Martínez-Lacaci, I. (2014). Role of receptor tyrosine kinases and their ligands in glioblastoma. *Cells* **3**, 199-235. doi:10.3390/cells3020199

DeLano, W. L. (2002). The PyMOL molecular graphics system on world wide web. http://www.pymol.org.

Deng, H., Lin, Y., Badin, M., Vasilcanu, D., Strömberg, T., Jernberg-Wiklund, H., Sehat, B. and Larsson, O. (2011). Over-accumulation of nuclear IGF-1 receptor in tumor cells requires elevated expression of the receptor and the SUMO-conjugating enzyme Ubc9. *Biochem. Biophys. Res. Commun.* **404**, 667-671. doi:10.1016/j.bbrc.2010.12.038

Farabaugh, S. M., Boone, D. N. and Lee, A. V. (2015). Role of IGF1R in breast cancer subtypes, stemness, and lineage differentiation. *Front. Endocrinol. (Lausanne)* **6**, 59. doi:10.3389/fendo.2015.00059

Gallois-Montbrun, S., Schneider, B., Chen, Y., Giacomoni-Fernandes, V., Mulard, L., Morera, S., Janin, J., Deville-Bonne, D. and Veron, M. (2002). Improving nucleoside diphosphate kinase for antiviral nucleotide analogs activation. *J. Biol. Chem.* **277**, 39953-39959. doi:10.1074/jbc.M206360200

Girnita, L., Worrall, C., Takahashi, S.-I., Seregard, S. and Girnita, A. (2014). Something old, something new and something borrowed: emerging paradigm of insulin-like growth factor type 1 receptor (IGF-1R) signaling regulation. *Cell. Mol. Life Sci.* **71**, 2403-2427. doi:10.1007/s00018-013-1514-y

Goldman, J. W., Mendenhall, M. A. and Rettinger, S. R. (2016). Hyperglycemia associated with targeted oncologic treatment: mechanisms and management. *Oncologist* **21**, 1326-1336. doi:10.1634/theoncologist.2015-0519

Hakuno, F. and Takahashi, S.-I. (2018). 40 YEARS OF IGF1: IGF1 receptor signaling pathways. *J. Mol. Endocrinol.* **61**, T69-T86. doi:10.1530/JME-17-0311

Hua, H., Kong, Q., Yin, J., Zhang, J. and Jiang, Y. (2020). Insulin-like growth factor receptor signaling in tumorigenesis and drug resistance: a challenge for cancer therapy. *J. Hematol. Oncol.* **13**, 64. doi:10.1186/s13045-020-00904-3

Jamwal, G., Singh, G., Dar, M. S., Singh, P., Bano, N., Syed, S. H., Sandhu, P., Akhter, Y., Monga, S. P. and Dar, M. J. (2018). Identification of a unique loss-of-function mutation in IGF1R and a crosstalk between IGF1R and Wnt/β-catenin signaling pathways. *Biochim. Biophys. Acta Mol. Cell Res.* **1865**, 920-931. doi:10.1016/j.bbamcr.2018.03.013

King, E. R. and Wong, K.-K. (2012). Insulin-like growth factor: current concepts and new developments in cancer therapy. *Recent Pat. Anticancer. Drug Discov.* **7**, 14-30. doi:10.2174/157489212798357930

Li, J., Choi, E., Yu, H. and Bai, X.-C. (2019). Structural basis of the activation of type 1 insulin-like growth factor receptor. *Nat. Commun.* **10**, 4567. doi:10.1038/s41467-019-12564-0

Lin, S.-B., Zhou, L., Liang, Z.-Y., Zhou, W.-X. and Jin, Y. (2017). Expression of GRK2 and IGF1R in hepatocellular carcinoma: clinicopathological and prognostic significance. *J. Clin. Pathol.* **70**, 754-759. doi:10.1136/jclinpath-2016-203998

Mills, J. V., Osher, E., Rieunier, G., Mills, I. G. and Macaulay, V. M. (2021). IGF-1R nuclear import and recruitment to chromatin involves both alpha and beta subunits. *Discov. Oncol.* **12**, 13. doi:10.1007/s12672-021-00407-8

Ngo, M.-H. T., Jeng, H.-Y., Kuo, Y.-C., Diony Nanda, J., Brahmadhi, A., Ling, T.-Y., Chang, T.-S. and Huang, Y.-H. (2021). The role of IGF/IGF-1R signaling in hepatocellular carcinomas: stemness-related properties and drug resistance. *Int. J. Mol. Sci.* **22**, 1931. doi:10.3390/ijms22041931

Packham, S., Warsito, D., Lin, Y., Sadi, S., Karlsson, R., Sehat, B. and Larsson, O. (2015). Nuclear translocation of IGF-1R via p150Glued and an importin-β/RanBP2-dependent pathway in cancer cells. *Oncogene* **34**, 2227-2238. doi:10.1038/onc.2014.165

Pautsch, A., Zoephel, A., Ahorn, H., Spevak, W., Hauptmann, R. and Nar, H. (2001). Crystal structure of bisphosphorylated IGF-1 receptor kinase. *Structure* **9**, 955-965. doi:10.1016/S0969-2126(01)00655-4

Sehat, B., Tofigh, A., Lin, Y., Trocme, E., Liljedahl, U., Lagergren, J. and Larsson, O. (2010). SUMOylation mediates the nuclear translocation and signaling of the IGF-1 receptor. *Sci. Signal.* **3**, ra10-ra10. doi:10.1126/scisignal.2000628

Simpson, A., Petnga, W., Macaulay, V. M., Weyer-Czernilofsky, U. and Bogenrieder, T. (2017). Insulin-like growth factor (IGF) pathway targeting in cancer: role of the igf axis and opportunities for future combination studies. *Target. Oncol.* **12**, 571-597. doi:10.1007/s11523-017-0514-5

Torres, A. M., Forbes, B. E., Aplin, S. E., Wallace, J. C., Francise, G. L. and Norton, R. S. (1995). Solution structure of human insulin-like growthfactor II. Relationship to receptor and binding protein interactions. *J. Mol. Biol.* **248**, 385-401.

Ullrich, A., Gray, A., Tam, A. W., Yang-Feng, T., Tsubokawa, M., Collins, C., Henzel, W., Le Bon, T., Kathuria, S. and Chen, E. (1986). Insulin-like growth factor I receptor primary structure: comparison with insulin receptor suggests structural determinants that define functional specificity. *EMBO J.* **5**, 2503-2512. doi:10.1002/j.1460-2075.1986.tb04528.x

Werner, H. and Bruchim, I. (2009). The insulin-like growth factor-I receptor as an oncogene. *Arch. Physiol. Biochem.* **115**, 58-71. doi:10.1080/13813450902783106

Yin, D., Sleight, B., Alvey, C., Hansson, A. G. and Bello, A. (2013). Pharmacokinetics and pharmacodynamics of figitumumab, a monoclonal antibody targeting the insulin-like growth factor 1 receptor, in healthy participants. *J. Clin. Pharmacol.* **53**, 21-28. doi:10.1177/0091270011432934

Yuan, J., Yin, Z., Tao, K., Wang, G. and Gao, J. (2018). Function of insulin-like growth factor 1 receptor in cancer resistance to chemotherapy. *Oncol. Lett.* **15**, 41-47.